# Scaling single-wavelength optical interconnects to 180 Gb/s with PAM-M and pulse shaping

Stefanos Dris*[a], Paraskevas Bakopoulos[a], Nikolaos Argyris[a], Christos Spatharakis[a], Hercules Avramopoulos[a]
[a]Photonics Communications Research Laboratory, National Technical University of Athens, Iroon Polytechneiou 9, 15780 Zografou, Greece

## ABSTRACT

Faced with surging datacenter traffic demand, system designers are turning to multi-level optical modulation with direct detection as the means of reaching 100 Gb/s in a single optical lane; a further upgrade to 400 Gb/s is envisaged through wavelength-multiplexing of multiple 100 Gb/s strands. In terms of modulation formats, PAM-4 and PAM-8 are considered the front-runners, striking a good balance between bandwidth-efficiency and implementation complexity. In addition, the emergence of energy-efficient, high-speed CMOS digital-to-analog converters (DACs) opens up new possibilities: Spectral shaping through digital filtering will allow squeezing even more data through low-cost, low-bandwidth electro-optic components.

In this work we demonstrate an optical interconnect based on an EAM that is driven directly with sub-volt electrical swing by a 65 GSa/s arbitrary waveform generator (AWG). Low-voltage drive is particularly attractive since it allows direct interfacing with the switch/server ASIC, eliminating the need for dedicated, power-hungry and expensive electrical drivers. Single-wavelength throughputs of 180 and 120 Gb/s are experimentally demonstrated with 60 Gbaud optical PAM-8 and PAM-4 respectively. Successful transmission over 1250 m SMF is achieved with direct-detection, using linear equalization via offline digital signal processing in order to overcome the strong bandwidth limitation of the overall link (~20 GHz). The suitability of Nyquist pulse shaping for optical interconnects is also investigated experimentally with PAM-4 and PAM-8, at a lower symbol rate of 40 Gbaud (limited by the sampling rate of the AWG). To the best of our knowledge, the rates achieved are the highest ever using optical PAM-M formats.

**Keywords:** Optical interconnects, PAM-4, PAM-8, pulse shaping, digital equalization

## 1. INTRODUCTION

Cloud applications, video content and the Internet of Things are driving datacenter traffic on a steep trajectory of growth. Sustained compound-annual-growth rates (CAGR) reaching 25% are expected for the coming years with no signs of decline for the foreseeable future[1], putting optical interconnects in the spotlight. While 100 Gb/s interfaces based on four parallel 25 Gb/s lanes were recently commercialized, migration to 400 Gb/s is urgently sought to keep pace with surging demand. First deployments apply 16 parallel 25 Gb/s lanes in a CDFP form factor to deliver 400 Gb/s with currently available optoelectronics. Although endorsed by a niche of performance-oriented early adopters, this approach comes with inherent limitations in terms of module size and power consumption[2]. Datacenter equipment suppliers are in consent that optical component count and the associated packaging is the dominant cost driver in optical interconnects[3], thereby a four-lane solution is pursued for migrating from current 100 Gb/s systems to 400 Gb/s and beyond, motivating research towards single-lane 100 Gb/s solutions.

Serial 100 Gb/s connectivity presents a formidable challenge, as it requires state-of-the-art high-bandwidth electronics, optics and printed circuit boards (PCBs) which currently struggle to cope with the extremely cost-sensitive requirements of the datacenter ecosystem. To circumvent this obstacle, higher-order modulation (HOM) is gaining momentum[4,5]. Providing more bits-per-symbol, HOM decouples the aggregate bitrate of the optical interconnect link with the speed capabilities of available CMOS nodes and the bandwidth of commodity optics such as DMLs and EMLs. Thus, lane speed can increase gracefully without being bound with the scaling curve of the associated components. A wide gamut of

*sdris@mail.ntua.gr; http://photonics.ntua.gr

Next-Generation Optical Networks for Data Centers and Short-Reach Links III, edited by Atul K. Srivastava,
Proc. of SPIE Vol. 9775, 977506 · © 2016 SPIE · CCC code: 0277-786X/16/$18 · doi: 10.1117/12.2208876

HOM solutions has been proposed for single-lane 100 Gb/s interconnects, with the main focus put on intensity modulation with direct detection (IM/DD) by virtue of its simpler implementation. Reported approaches seek to strike the optimum balance between spectral efficiency and feasibility for large-scale deployment in datacenter settings, and span from pulse-amplitude modulation (PAM) to quaternary amplitude modulation (QAM) on a single sub-carrier and its sibling carrier-less amplitude phase (CAP) modulation, extending all the way to multi-carrier approaches like discrete multi-tone (DMT)[2,4].

Among the various HOM options for serial 100G, PAM-4 is attracting particular interest for deployment in commercial systems. Although less spectrally efficient than the rest, PAM-4 is being endorsed by the 400 Gb/s Physical Layer taskforce[6] due to its lower implementation complexity and its precedent in standards (IEEE 802.3bj™). Single-lane 140 Gb/s PAM-4 transmission over 20 km was demonstrated in the low-dispersion 1310 nm spectral region (O-band) using faster-than-Nyquist direct detection[7]. Despite the more pronounced effects of chromatic dispersion in the 1550 nm region (C-band), the vast availability of optical components is stimulating commercial interest[8]. Transmission of 112 Gb/s PAM-4 channels was reported in the C-band over 80 km of single-mode fiber using erbium-doped fiber amplification and maximum likelihood sequence estimator (MLSE) equalization at the receiver[9]. As a means to avoid complex DSP, a higher bandwidth approach was reported using a 50 GHz electro-absorption modulator (EAM) to transmit 112 Gb/s over 2 km of single-mode fiber (SMF), requiring only a 3-tap Feed-Forward Equalizer (FFE) equalizer[10]. Besides the limited availability of broadband electro-optic components, such a wide-bandwidth approach comes with a number of implications to the overall system, the most salient of which concern the strict RF requirements for the PCB, the faster accumulation of dispersion that limits optical reach and the higher sampling rate required at the receiver's digital-to-analogue converter (DAC) due to the higher frequency components of the signal. To bypass these shortcomings, methods for enhancing the signal's spectral efficiency are pursued. Nyquist pulse-shaping is proposed as a means of band-limiting the PAM-4 signal with minimum inter-symbol interference. The concept was verified with the transmission of 102.4 Gb/s Nyquist PAM-4 over 2 km of single-mode fiber, using a 35 GHz Mach-Zehnder modulator[11]. As an alternative, higher-order PAM is also investigated; notably PAM-8, as it provides an integer number of bits/symbol and could serve as a natural migration path from PAM-4 systems with reasonable added complexity. Generation of 100 Gb/s PAM-8 was demonstrated with an electro-absorption modulated laser operating in the O-band[12]. In the C-band, a 105 Gb/s transmitter was demonstrated in[13] with an integrated transmitter based on an InP Mach-Zehnder modulator, whereas recently we reported the transmission of 120 Gb/s PAM-8 over 2 km of single-mode fiber using an off-the-shelf electro-absorption modulator with 24.3 GHz bandwidth[14].

In this paper we demonstrate a single-wavelength optical interconnect link operating at 60 Gbaud, achieving 180 Gb/s and 120 Gb/s throughput over 1250 m of standard SMF with PAM-8 and PAM-4 modulation respectively. To the best of our knowledge, the rates reported are the highest ever demonstrated experimentally using optical PAM-M in the C-band. The optical interconnect is based on off-the-shelf components combined with linear equalization through digital signal processing (DSP) at the receiver to compensate for the strong bandwidth limitations of the overall link. The effect of root raised cosine (RRC) pulse shaping for PAM-4 and PAM-8 is investigated both experimentally and numerically at 40 Gbaud (limited by the sampling rate of the data generator). A fully digital implementation is pursued for the generation and detection of the PAM signals, which capitalizes on the availability of energy-efficient CMOS DAC and ADC cores operating at 65 GSa/s [15-17]. To address the discrepancy between the low-voltage capability of CMOS DACs and the driving requirements of typical EMLs and DMLs (e.g. 1.7 $V_{pp}$ in[7], 2 $V_{pp}$ in[12]), which entails the use of a driver amplifier, we extend on our prior work[14] and drive the off-the-shelf electro-absorption modulator directly by the CMOS data converter at sub-volt electrical swing. Eliminating the driver amplifier is pivotal towards reducing power consumption and bill of materials in optical interconnects, while enabling close integration of the CMOS switch/server ASIC with the optics.

## 2. PAM-M SIMULATIONS

Simulations of an optical interconnect employing IM/DD and PAM were carried out using VPItransmissionMaker[18]. The goal of this exercise was to gauge the performance improvement when using pulse-shaping at the transmitter, in bandlimited channels. 40 Gbaud was the chosen symbol rate, reflecting the scheme followed in the subsequent experiments; the latter was chosen due to the need for transmitter-side oversampling to provide adequate pulse shaping (the AWG used for electrical data generation was capable of up to 65 GSa/s, and thus the oversampling rate at 40 Gbaud was 1.625 at most).

## 2.1 Simulation setup and methodology

Figure 1 is the schematic of the link used to simulate transmission of 40 Gbaud PAM-4 optical signals over SMF. The multi-level electrical signals were generated in MATLAB and supplied to an ideal EAM that modulated the light from a 0 dBm continuous wave (CW) 1550 nm laser. Two different pulse shapes were used: 'Unshaped' (i.e. conventional NRZ signaling) and Root Raised Cosine with a roll-off factor $\alpha$=0.1.

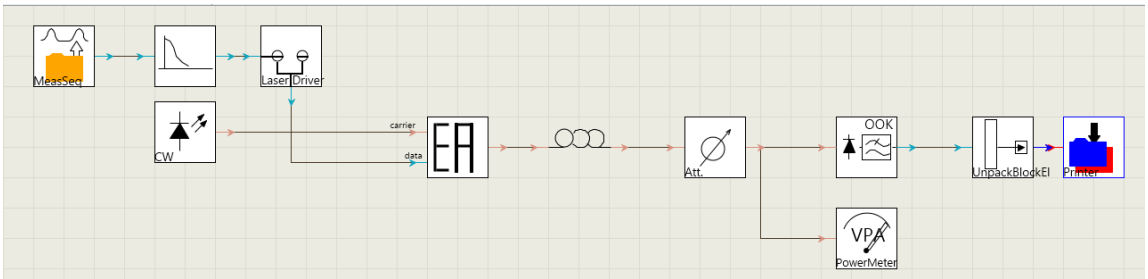


Figure 1. VPItransmissionMaker simulation setup for the 40 Gbaud PAM-4 optical interconnect.

In order to emulate the case of an electrical DAC whose output swing is confined to a finite range, the amplitude of the input electrical signals were both set to 1 $V_{pk\text{-}pk}$. In practice this meant that, due to the overshoot which is inherent in RRC pulses, the signal power for the RRC pulse-shaped signal was lower than that of the unshaped case. It follows that the resulting optical modulation amplitude (OMA) of the RRC-shaped signal is lower than that of the unshaped one (OMA being defined as the difference in power between the highest and lowest levels of the PAM-4 signal). This can be observed in Figure 2, where eye diagrams are plotted for the two cases of input electrical signals.

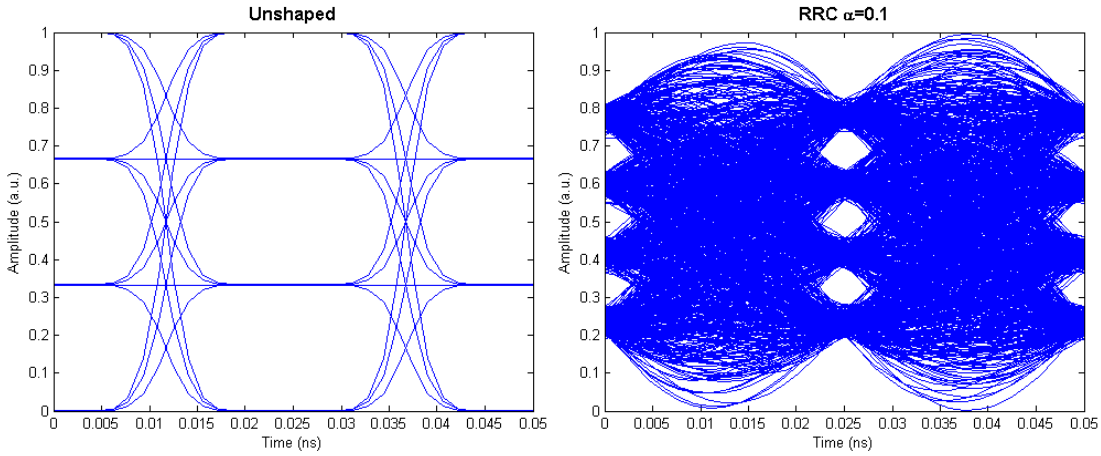


Figure 2. Eye diagrams of the unshaped (left) and RRC-shaped (right) PAM-4 electrical signals used in the simulations.

The overall bandwidth limitation was emulated at the transmitter by inserting an analog electrical filter at the input of the EAM. The following frequency response models were used: (a) 8$^{th}$ order Chebyshev Type I with 1 dB ripple in the passband and 22 GHz 3-dB bandwidth, (b) 8$^{th}$ order Chebyshev Type II with 22 GHz 3-dB bandwidth, and (c) 8$^{th}$ order Chebyshev Type II with 40 GHz 3-dB bandwidth. These were chosen so as to compare the effects on the different pulse-shapes of a smooth passband response (Chebyshev II) vs one with ripple (Chebyshev I), as well as of a steep transition band (Chebyshev I) vs a smoother roll-off (Chebyshev II). Finally, the Chebyshev Type II channel with 40 GHz 3-dB bandwidth was used to compare performance against the bandlimited cases (22 GHz). Figure 3 shows the frequency responses of the 3 electrical filters employed. Included in the same plot are the Power Spectral Densities (PSDs) corresponding to the unshaped and RRC electrical signals.

The optical signal was then launched into 4 lengths of SMF (500, 1000, 2000 and 4000 m). A variable optical attenuator (VOA) was placed just before the linear photoreceiver in order to allow sweeping of the received optical power, and obtain BER plots as a function of Rx power. Each simulation run lasted 20 μs, enough to send and receive ~800 000 symbols (=1 600 000 bits when using PAM-4).

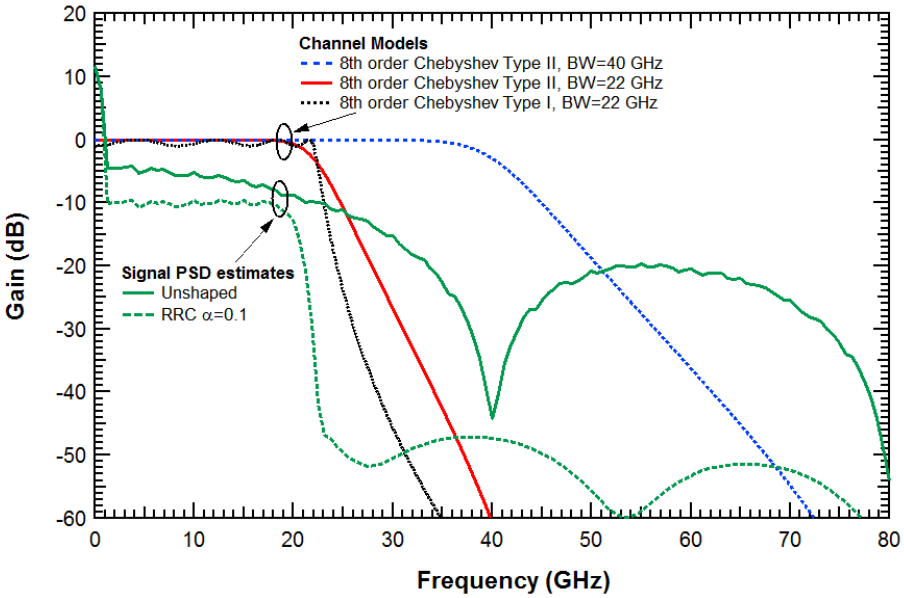


Figure 3. Frequency responses of the channel models used in the simulations (Chebyshev Type I with 22 GHz 3 dB bandwidth and 0.1 dB passband ripple, Chebyshev Type II with 22 and 40 GHz 3 dB bandwidths). Also shown are the PSDs of the 40 Gbaud PAM-4 electrical signals for the unshaped (solid green line), and RRC with $\alpha$=0.1 pulse-shaped (dotted green line) cases.

The received optical signals were converted to electrical by a linear photoreceiver, after which they were digitized and processed in MATLAB. The receiver DSP is shown in Figure 4 and included resampling to 4 samples/symbol, matched RRC Rx filtering (only for the RRC-shaped case), symbol clock recovery using the square timing algorithm, symbol-spaced linear equalization, thresholding and symbol detection, and finally, decoding and bit error counting. The equalizer coefficients were obtained by employing an adaptive FFE structure operating in decision-directed mode with the normalized least mean squares (LMS) algorithm, at zero receiver attenuation (i.e. at the highest Rx optical power). The number of taps employed was different in each case, and was chosen so as to minimize the mean square error (MSE) of the estimation. In practice, this meant that the number of taps was successively increased, the coefficients were adapted, and the final number of taps selected was the one beyond which no significant improvement in MSE could be obtained. The BER for each run was then obtained with the fixed equalizer coefficients determined by the process just described.

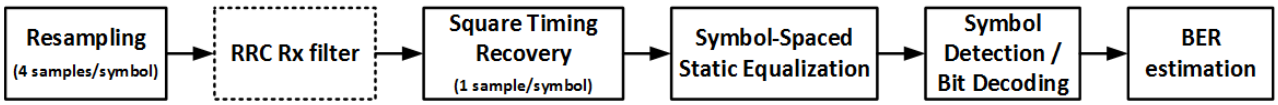


Figure 4. Receiver DSP implemented in MATLAB for the PAM-4 simulations. The RRC matched Rx filter was only used for the RRC pulse-shaped signal.

### 2.2 Simulation results and discussion

The left column of Figure 5 shows all BER curves obtained as a function of received optical power, SMF transmission lengths, channel response models and pulse-shaping. On the right, the required optical power to achieve a BER of $1{\cdot}10^{-3}$ is plotted against SMF transmission length. The number of equalizer taps used in the simulations of the 500 m length of fiber is given in Table 1 for each channel model (the other lengths of fiber show the same trend, and are thus not shown).

Looking at the BER plots as a function of Rx optical power, the RRC-shaped signal outperforms the unshaped signal for the Chebyshev I channel response, requiring ~0.8 dB less Rx power for a BER of $1{\cdot}10^{-3}$. This is despite the fact that the signal power of the RRC signal had to be 'backed-off' to avoid clipping due to overshoots in the transitions, as explained in the previous section.

Table 1. Number of equalizer taps used in the simulation runs. Only the runs corresponding to the 500 m fiber length are shown.

| Channel Model | Number of Equalizer Taps | |
|---|---|---|
| | RRC $\alpha$=0.1 | Unshaped |
| Chebyshev I – 22 GHz | 27 | 37 |
| Chebyshev II – 22 GHz | 17 | 11 |
| Chebyshev II – 40 GHz | 5 | 9 |

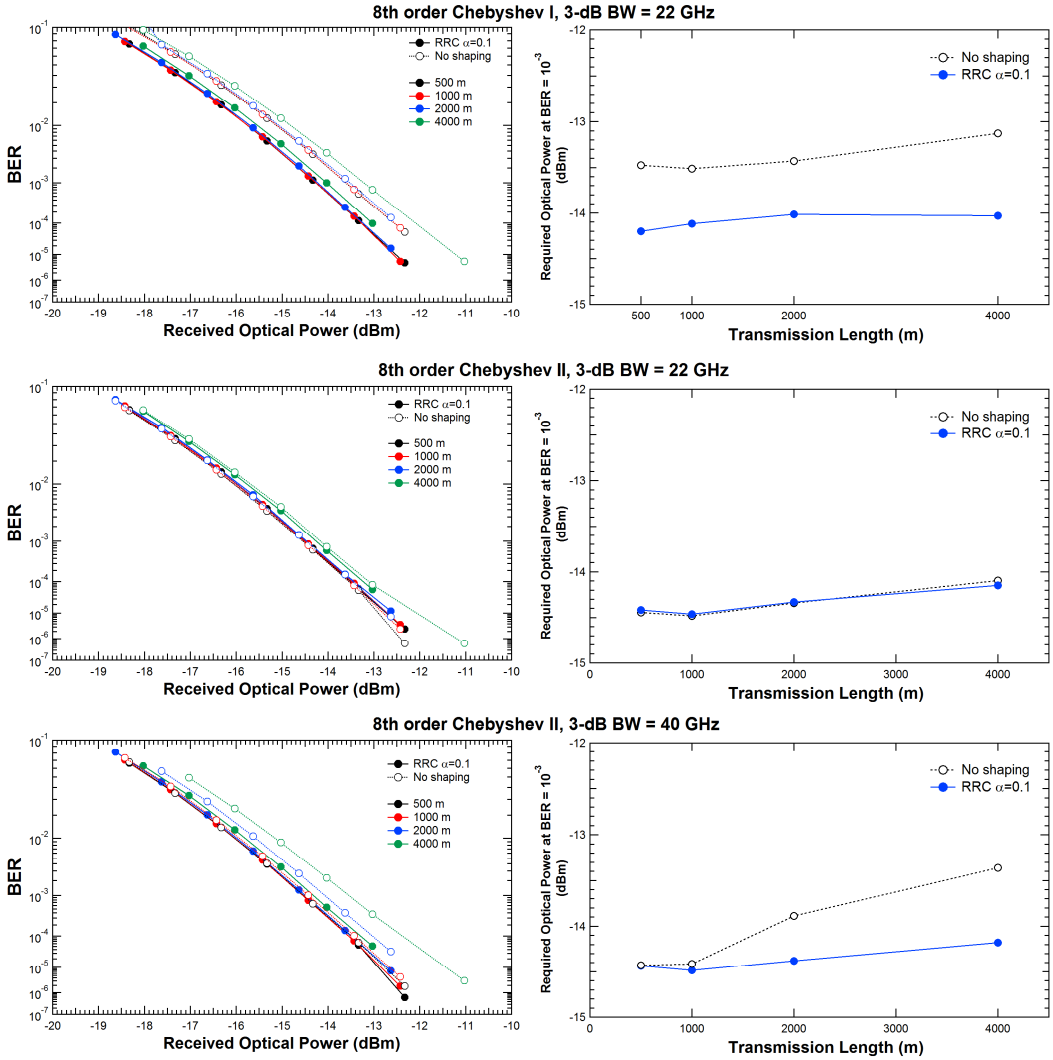


Figure 5. BER plots obtained as a function of received optical power (left column), for the Chebyshev I 22 GHz (top row), Chebyshev II 22 GHz (middle row), and Chebyshev II 40 GHz (bottom row) channel responses. The solid lines with the solid markers correspond to the RRC-shaped signals, while the dotted lines with hollow markers correspond to the unshaped ones. BER curves were obtained for 4 different lengths of SMF, as indicated by the different line colors. In the right column, the required optical power at the Rx to achieve a BER of $1 \cdot 10^{-3}$ is plotted as a function of SMF length, for each channel and both types of signal (RRC and unshaped).

This is not the case for the Chebyshev II 22 GHz channel, where the performance difference between the two types of signal is negligible. Clearly, the sharp transition band of the Chebyshev I response degrades the unshaped PAM-4 signal much more than does the smoother roll-off of the Chebyshev II channel. It follows that employing RRC pulse shaping is only advantageous in the case of bandlimited channels whose transfer functions roll-off sharply.

As far as the Chebyshev II 40 GHz response is concerned, only the 500 and 1000 m SMF lengths yield similar results for both cases. When the length is increased, the unshaped signal suffers a degradation penalty. This is undoubtedly the effect of chromatic dispersion, which is more pronounced when the spectral content of the signal is larger, and cannot be adequately mitigated by the linear equalizer of a direct-detection digital receiver (since there is no optical phase information available). This leads to an interesting observation: In long optical interconnects of 2 km or more, high-baudrate signals (≥40 Gbaud) perform better if they are bandlimited; whether this is intentional through the use of pulse-shaping, or an unintended consequence of the response of the channel.

## 3. PAM-M EXPERIMENTS

### 3.1 Experimental setup

Figure 6 shows the experimental setup for the PAM-4 and PAM-8 optical interconnect. 40 and 60 Gbaud electrical signals were generated with an 8-bit, 65 GSa/s arbitrary waveform generator (AWG) providing a single-ended output, yielding bitrates of 80 and 120 Gb/s with PAM-4, and 120 and 180 Gb/s with PAM-8. The repeating pattern length was $2^9$ symbols. In order to overcome the limited analog bandwidth of the AWG (~20-22 GHz at the 3 dB point), RRC pulse-shaping with $\alpha$=0.1 was employed in the case of the 40 Gbaud PAM-M signals. This was not possible with the 60 Gbaud signals, since the 65 GSa/s sampling rate of the AWG did not provide enough oversampling for pulse shaping.

The multi-level AWG signals were directly introduced to an off-the-shelf 40 Gb/s electro-absorption modulator, exhibiting 3-dB and 6-dB electro-optic bandwidths of 24.3 GHz and 40 GHz respectively. No RF amplification was employed; the voltage swings (including overshoots) of the 40 Gbaud PAM-4 and PAM-8 signals were 930 $mV_{pk-pk}$ and 840 $mV_{pk-pk}$ respectively. For the 60 Gbaud PAM-4 and PAM-8, the swings were measured at 730 $mV_{pk-pk}$ and 780 $mV_{pk-pk}$. This meant that the achievable modulation depth at the EAM was limited to less than 10 dB. The EAM was powered by a 7.8 dBm continuous wave (CW) optical signal at 1560 nm, provided by a DFB laser with 145 dB/Hz relative intensity noise (RIN). The generated multi-level optical signal was transmitted through a 1250 m spool of standard SMF. An off-the-shelf 40 Gb/s photoreceiver was used for signal detection, consisting of a waveguide-integrated pin-photodiode (PD) and a transimpedance amplifier (TIA) with limiting output buffer. The photoreceiver exhibited a 3 dB bandwidth of 35 GHz, 0.6 A/W responsivity, 500 V/W conversion gain and -12 dBm sensitivity. Due to the limiting operation of the available photoreceiver, operation at low received power was necessary in order to avoid nonlinear distortion. A variable optical attenuator was placed at the input of the photoreceiver, to allow sweeping of the received optical power. The electrical signals from the photoreceiver were sampled at 80 GSa/s using a real-time oscilloscope with analog bandwidth 33 GHz.

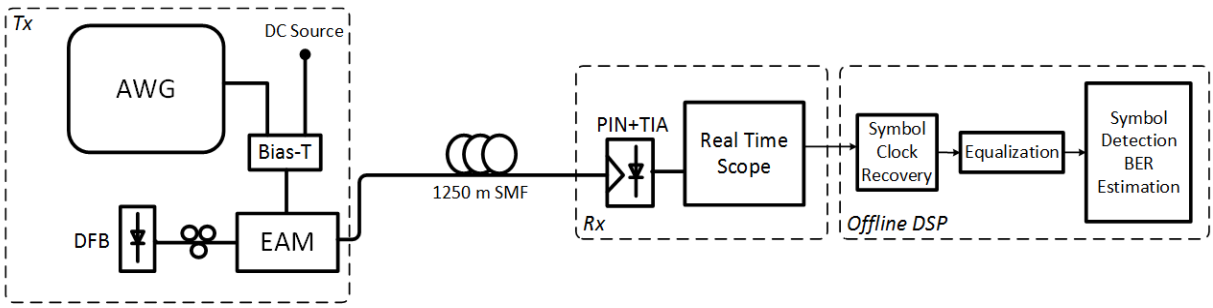


Figure 6. Experimental setup of the EAM-based optical interconnect.

### 3.2 DSP processing

The captured data were processed with offline DSP in order to assess the link's performance. The same DSP procedure that was used for the simulations was also followed for processing the experimental data (Figure 4). The discretized signals were first resampled to 4 samples/symbol. In the case of RRC-shaped signals, a matched RRC Rx filter was applied, after which the square timing algorithm was employed to recover the symbol clock. The resulting

1 sample/symbol at the best sampling point was then fed to a symbol-spaced FFE structure to estimate the channel response. The equalizer weights were first adapted with a known training pattern and the normalized LMS algorithm. Once the estimation error was sufficiently minimized, the training process was stopped. The derived tap weights were then used to equalize the received data with a static FIR filter. It should be noted that coefficient adaptation was only performed at the highest available power (i.e. no attenuation). The resulting static equalizer was then applied to all other (lower) received optical powers. Further processing and analysis could then be performed on the equalized data sequences, including symbol detection and BER estimation with Gray encoding.

### 3.3 Results and discussion

In order to visualize the signal quality of the PAM-M signals, the probability density functions (PDFs) of the received symbol amplitudes were estimated and are plotted here. Figure 7 shows the AWG's electrical signals that were used as modulating inputs in the EAM (for 40 and 60 Gbaud PAM-4). It should be noted that an Rx RRC digital filter was applied in the case of the 40 Gbaud PAM-4 (the effect of which is included in the PDF shown), to complement the corresponding Tx-side RRC pulse-shaping filter. The bandwidth limitation of the analog electronic front end is especially evident in the 60 Gbaud signal, where there is overlap between the adjacent transmitted symbols. The evolution of signal quality can be tracked by looking at the optical outputs of the EAM in Figure 8 (with and without digital equalization for both symbol rates), and the (final) signals after transmission in 1250 m SMF and optoelectronic conversion in the photoreceiver (Figure 9). Figure 10, Figure 11 and Figure 12 show the corresponding PDFs for the RRC-shaped 40 and unshaped 60 Gbaud PAM-8 signals. For all PDFs, it is the highest available optical Rx power that is plotted.

As expected, the signal deteriorates progressively as it traverses each part of the link. There is symbol overlap even in the back-to-back PDFs as a result of the frequency response of the Tx components used, not just because of bandwidth limitation, but also due to severe passband ripple. It is clear that digital equalization is necessary in order to invert the channel's effects and obtain acceptable BER performance. Though the number of equalizer taps used varied from case to case, the PAM-4 signals at 40 Gbaud typically required over 200 taps to achieve the performance shown here (>400 for the 60 Gbaud signals). While this is a large number of taps introducing complexity for the digital receiver, it is a product of the particular channel which was far from ideal. The simulation results indicate that if the overall channel response is smoother, the severe bandwidth limitation can be overcome with much fewer equalizer taps.

The BERs as a function of Rx optical power were measured in back-to-back configuration, and after 1250 m transmission. Figure 13 shows the curves obtained for 40 Gbaud RRC and unshaped 60 Gbaud PAM-4 (left) and 40 Gbaud RRC and unshaped 60 Gbaud PAM-8 (right). In all cases, the transmission penalty is less than ~1 dB, corroborating the simulation results which did not show significant deterioration due to chromatic dispersion for bandlimited signals. Indeed, the lowest BERs obtained were limited due to the available Rx optical power.

The maximum available power for the 40 Gbaud RRC-shaped PAM-4 was at -6.3 dBm, with a corresponding BER of $4.4 \cdot 10^{-7}$. This would allow the use of a very simple and low overhead (3%) code such as Reed Solomon (528,514) [19]. 60 Gbaud PAM-4 after transmission performs worse in comparison, but is still below the FEC threshold ($1 \cdot 10^{-3}$) required by a relatively simple hard-decision FEC such as BCH(3456,3084) with 11% overhead[19]. The same code can be used for the 40 Gbaud RRC PAM-8, which, at the highest received power after transmission (-5.8 dBm), achieves a BER of $5.4 \cdot 10^{-4}$. As expected, successful transmission of 60 Gbaud PAM-8 (180 Gb/s on a single-wavelength) can only be achieved with much stronger FEC; a soft-decision code with 20% overhead and pre-FEC BER threshold of $\sim 2 \cdot 10^{-2}$ such as the one used for telecom systems would be needed[20].

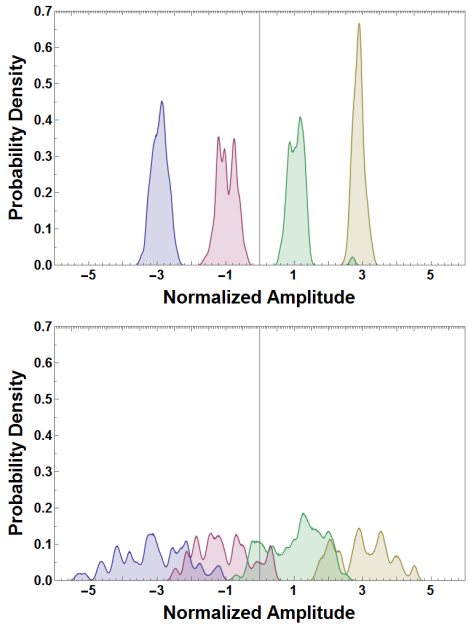


Figure 7. Amplitude PDFs of the electrical signals without equalization at the output of the AWG for RRC 40 Gbaud (top) and unshaped 60 Gbaud (bottom) PAM-4. In the case of 40 Gbaud PAM-4 for which pulse-shaping was used at the Tx, the PDF shown here includes the effect of a matched Rx RRC digital filter.

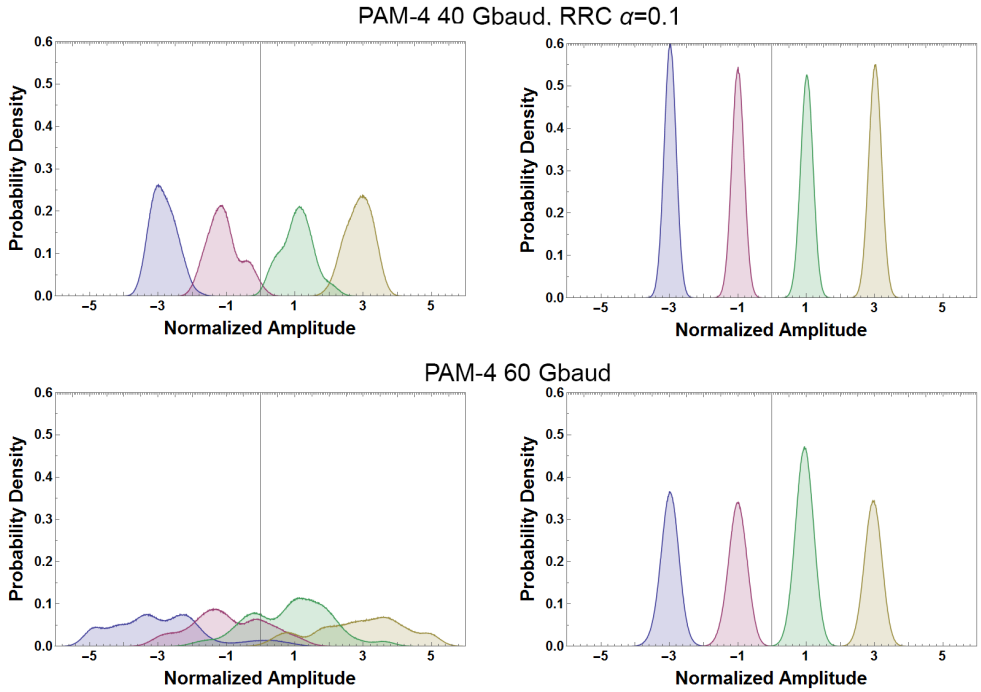


Figure 8. Amplitude PDFs before (left column) and after (right column) equalization at the highest received power for RRC-shaped 40 Gbaud (top row) and unshaped 60 Gbaud (bottom row) PAM-4 optical back-to-back measurements.

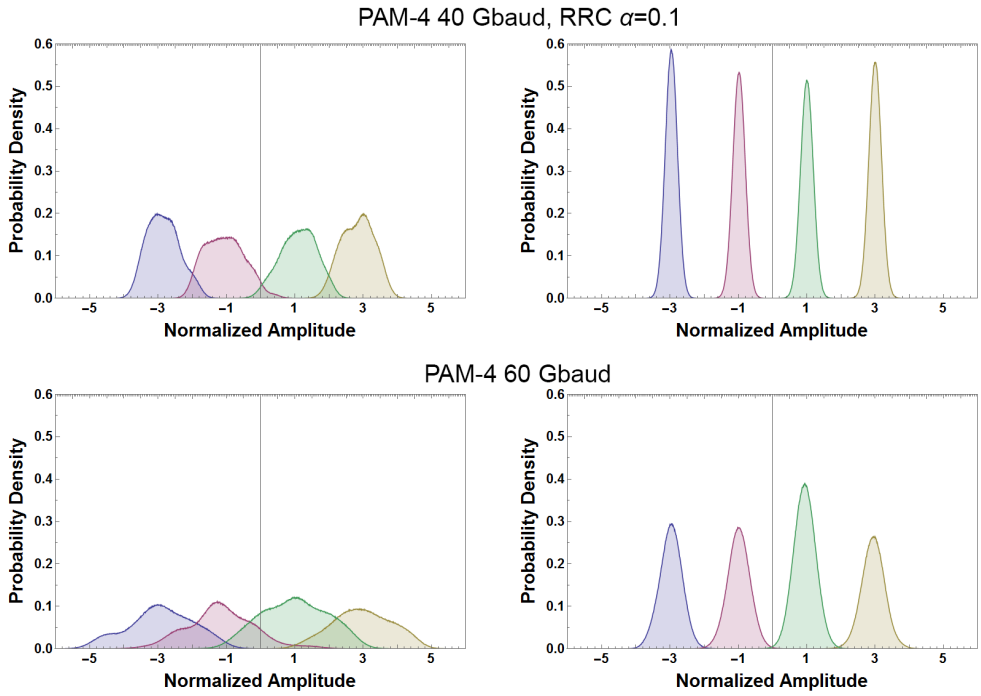


Figure 9. Amplitude PDFs before (left column) and after (right column) equalization at the highest received power for RRC-shaped 40 Gbaud (top row) and unshaped 60 Gbaud (bottom row) PAM-4 transmission over 1250 m SMF.

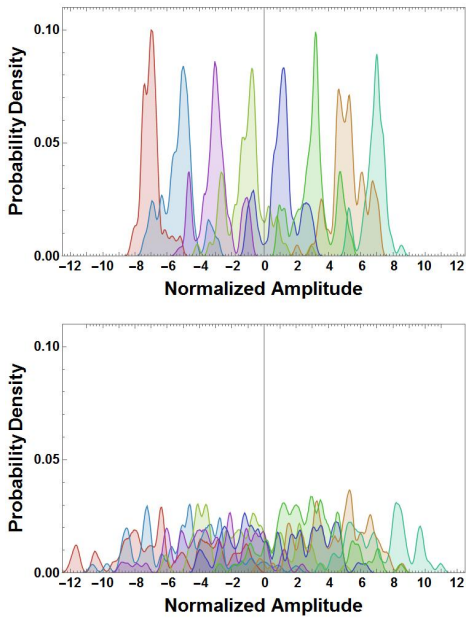


Figure 10. Amplitude PDFs of the electrical signals without equalization at the output of the AWG for RRC 40 Gbaud (top) and unshaped 60 Gbaud (bottom) PAM-8. In the case of 40 Gbaud PAM-8 for which pulse-shaping was used at the Tx, the PDF shown here includes the effect of a matched Rx RRC digital filter.

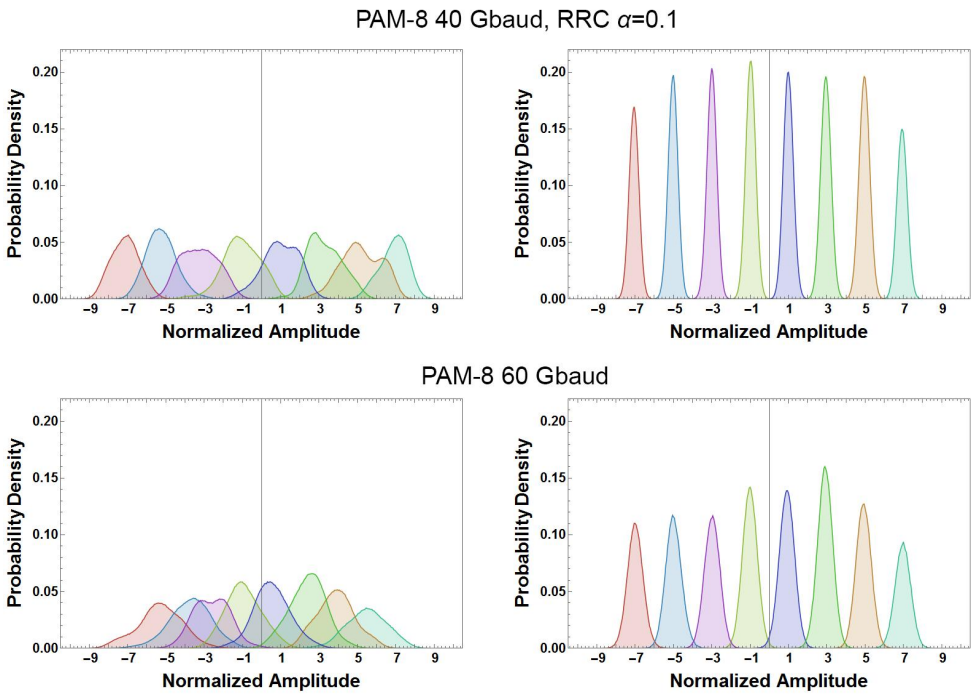


Figure 11. Amplitude PDFs before (left column) and after (right column) equalization at the highest received power for RRC-shaped 40 Gbaud (top row) and unshaped 60 Gbaud (bottom row) PAM-4 optical back-to-back measurements.

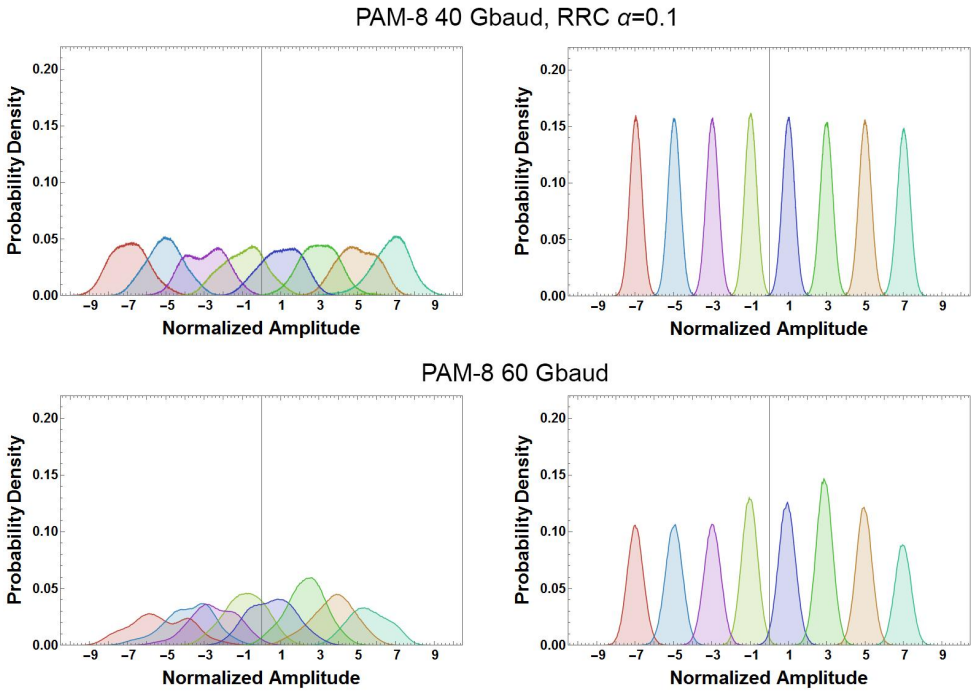


Figure 12. Amplitude PDFs before (left column) and after (right column) equalization at the highest received power for RRC-shaped 40 Gbaud (top row) and unshaped 60 Gbaud (bottom row) PAM-8 transmission over 1250 m SMF.

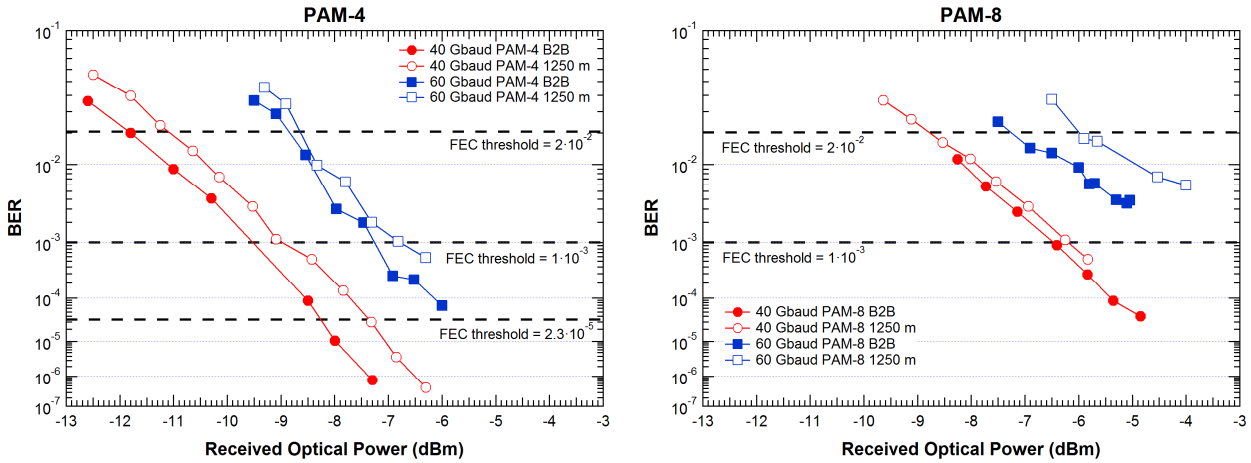


Figure 13. BER as a function of received optical power obtained experimentally for RRC-shaped 40 Gbaud (red circles) and unshaped 60 Gbaud (blue squares) PAM-4 (left) and PAM-8 (right), in back to back configuration (solid markers), and after transmission over 1250 m SMF (hollow markers).

## 4. CONCLUSIONS

We have carried out successful transmission of single-wavelength 80 Gb/s PAM-4, 120 Gb/s PAM-4 and PAM-8, and 180 Gb/s PAM-8 over 1250 m SMF, aimed at optical links for intra-datacenter connectivity. Digital equalization at the receiver with a symbol-spaced FIR filter ensured that the effects of the severely bandlimited channel could be reversed, and operation below the FEC-limit could be achieved in all cases. System performance was limited by the power available at the receiver, as well as the constrained OMA arising from the low voltage swing of the multi-level signal driving the EAM. The sub-volt electrical driving scheme we have shown is achievable with state-of-the-art CMOS electronics found in switch or server ASICs, and does not require power-hungry linear RF modulator drivers. It is therefore very relevant for datacenter applications, where energy-efficiency is of primary importance.

## ACKNOWLEDGEMENTS

This work has received funding from the European Union's Horizon 2020 and FP7 research and innovation programs under grant agreements No 645212 (NEPHELE), No 318240 (PHOXTROT) and 318228 (MIRAGE). The manuscript reflects only the authors' view and the Commission is not responsible for any use that may be made of the information it contains. The authors gratefully acknowledge Keysight Technologies for providing the AWG.

## REFERENCES

[1] "Cisco Global Cloud Index: Forecast and Methodology, 2014–2019", Cisco, October 2015, http://www.cisco.com/c/en/us/solutions/collateral/service-provider/global-cloud-index-gci/Cloud_Index_White_Paper.pdf (31 January 2016).
[2] Lyubomirsky, I. and Ling, W. A., "Digital QAM Modulation and Equalization for High Performance 400 GbE Data Center Modules," Proc. OFC W1F.4 (2014).
[3] Bhatt, V., Dama, B., and Nicholl, G., "Update on Advanced Modulation for a Low Cost 100G Single Mode Fiber PMD," Proc. Next Generation 40 Gb/s and 100 Gb/s Optical Ethernet Study Group, (2012).
[4] Cole, C., Lyubomirsky, I., Ghiasi A. and Telang, V., "Higher-Order Modulation for Client Optics," IEEE Communications Magazine 51(3), 50-57 (2013).
[5] Apostolopoulos, D. et. al., "Photonic integration enabling new multiplexing concepts in optical board-to-board and rack-to-rack interconnects," Proc. SPIE 8991, Optical Interconnects XIV, 89910D (2014).
[6] IEEE P802.3bs 400 Gb/s Ethernet Task Force, 19 October 2015, http://www.ieee802.org/3/bs (31 January 2016).

[7] Zhong, K., et. al., “140-Gb/s 20-km Transmission of PAM-4 Signal at 1.3 μm for Short Reach Communications”, IEEE Photonics Technology Letters 27(16), 1757-1760 (2015).
[8] OpenOptics MSA, http://openopticsmsa.org (18 January 2016).
[9] Sadot, D., Dorman, G., Gorshtein, A., Sonkin, E., and Vidal, O., “Single channel 112Gbit/sec PAM4 at 56Gbaud with digital signal processing for data centers applications,” Optics Express 23(2), 991-997 (2015).
[10] Caillaud, C., et al., “Low cost 112 Gb/s InP DFB-EAM for PAM-4 2 km Transmission,” Proc. ECOC PDP1.5 (2015).
[11] Kikuchi, N. and Hirai, R., “Intensity-Modulated / Direct-Detection (IM/DD) Nyquist Pulse-Amplitude Modulation (PAM) Signaling for 100-Gbit/s/λ Optical Short-reach Transmission,” Proc. ECOC P4.12 (2014).
[12] Troppenz, U., et al., “1.3 μm Electroabsorption Modulated Lasers for PAM4/PAM8 single channel 100 Gb/s,” Proc. IPRM Th-B2-5 (2014).
[13] Saavedra, B. G., et. al., “First 105 Gb/s low power, small footprint PAM-8 impedance-engineered TOSA with InP MZ-modulator and customized driver IC using predistortion,” Proc OFC Th4E.4 (2015).
[14] Bakopoulos, P., Dris, S., Argyris, N., Tokas, K. and Avramopoulos, H., “120 Gb/s PAM-8 and 80 Gb/s PAM-4 Optical Interconnect with a Sub-Volt Driven EAM,” Proc ACP AS4D.4 (2015).
[15] Yan, W. Z., et. al., “100 Gb/s optical IM-DD transmission with 10G-class devices enabled by 65 GSamples/s CMOS DAC core,” Proc. OFC OM3H.1 (2013).
[16] “LEIA digital-to-analog converter,” Fujitsu Semiconductor Europe, 29 March 2012, http://www.fujitsu.com/downloads/MICRO/fme/documentation/c60.pdf (18 January 2016).
[17] “LUKE-ES analog-to-digital converter,” Fujitsu Semiconductor Europe, 29 March 2012, http://www.fujitsu.com/downloads/MICRO/fme/documentation/c63.pdf (18 January 2016).
[18] VPItransmissionMaker™ Optical Systems, http://www.vpiphotonics.com/Tools/OpticalSystems/
[19] Sakib, M. N., et al., “A Study of Error Correction Codes for PAM Signals in Data Centers Applications,” IEEE Photon. Technol. Lett., Vol. 25, no. 23, pp 2274-2277 (2013).
[20] Zhang, J., et al. “WDM Transmission of Single-Carrier 400G Based on Orthogonal OTDM 80-GBd PDM-8QAM,” IEEE Phot. Journal, Vol. 7, No. 4 (2015).